Condition Monitoring of Bearings in a Viaduct

C. H. Chew
Department of Mechanical & Production Engineering
Natinal University of Singapore
Kent Ridge Cresent, Singapore 0511

ABSTRACT: The bearings used under the viaducts of the mass rapid transit system are of the sealed type. Though this type of bearings is useful in preventing the elastomer from exposure to ultraviolet light and the elements, it has the drawback of preventing the visual inspection of the physical condition of the elastomer. By measuring the end displacements of the viaduct, we could correlate the peak-to-peak displacements with the elasticity of the elastomer of the bearings used. Analysis shows that the ballast stiffness has very little influence over the end displacements, and the variations of the end displacements are more affected by the stiffnesses of the bearings than the variation in passenger load.

1. INTRODUCTION

Elevated viaduct for the rapid transit system in Singapore consitutes a significant portion of the whole system. The ends of the viaduct rest on columns via bearings as shown in Fig. 1. The bearings are introduced[1] to allow for the movements and rotations of the viaduct relative to the columns. Also shown in Fig. 1 are the general dimensions of a typical viaduct. The train runs on ballasted track. Fig. 2 shows a schematic view of the bearings used. The elastomer is totally sealed by metal rings. This type of bearing prevents the elastomer from exposure to ultraviolet light and the elements and thus prolongs the useful life of the bearing. However, it has the drawback of preventing visual inspection of the physical condition of the elastomer.

Though this type of bearing may have useful life from 50 to 80 years[1], it is essential that periodic inspection of the elastomer be carried out. Failure of the bearings may have undesirable structural consequences. As presently installed, physical inspection could only be carried out by jacking up the viaduct. This process could only be carried out when the system is not in operation, and therefore inspection work could only be carried out for a four hour period in the early hours. This is not only costly but also not practical. As precautionary measure, the bearings could be replaced before the end of the useful life; however, it is very costly. If the bearings could be replaced only when needed to, potential saving of a few million dollars per year could also be realised. As such there is a need for an alternative means to monitor the physical condition of the bearings.

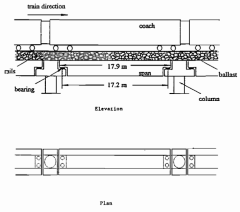

Figure 1. Elevated viaduct of rapid transit system.

2. VIBRATION MEASUREMENTS ON VIADUCT

Fig. 3 shows the configuration of the first three coaches of a 6-coach train. Each train rests on two bogies such as A1 and A2, B1 and B2, and so on. Each bogie carries two sets of wheels. As the train passes over a viaduct, the viaduct will be set into vibration. As such vibration measurements of the viaduct during a passage of the train could be used to monitor the condition of the bearings used on the viaduct; two parameters of the vibration, the acceleration and displacement signatures, were recorded and analysed during the passage of the train to determine whether the above parameters are suitable to condition monitor the physical condition of the bearings.

2.1 Acceleration Measurements

Accelerometers were placed on the underside of the ends of the viaduct at $x=0$ and $x=L_s$. $x=0$ is the end of the viaduct

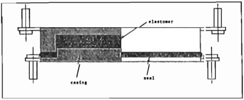

Figure 2. Schematic view of bearing.

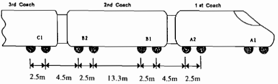

Figure 3. Configuration of the train.

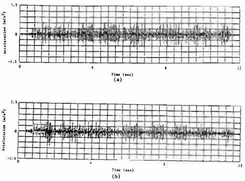

Figure 4. Acceleration signatures at (a) x=0, and (b)x=L_s.

where the train first enters the viaduct, while x=L_s is where the train leaves the viaduct. As the viaduct was quite near to a station, the speed of the train at the viaduct was about 58 km/h (15.9 m/s). At each bearing point, the train took about 9 sec to pass through. The acceleration signatures at x=0 and x=L_s were as shown in Fig. 4 .

The durations of the acceleration signatures were about 11 sec. This shows that the viaduct was set into vibration before the train has reached the viaduct and after it has left the viaduct. Furthermore, the time difference before significant acceleration signal was detected at x=L_s was about 0.4 sec later than at x=0. The time taken for the first set of wheels to travel the span of the viaduct was about 1.1 sec. This shows that before the first set of wheels was at a span, significant acceleration was experienced at x=L_s. It clearly indicates that the accelerations at the ends of the viaduct are much affected by movements of the neighbouring viaducts. From the above figures, we could estimate that the peak-to-peak acceleration during the passage of the train was about 30% higher than when the train was about to enter the viaduct and immediately after it had left the viaduct. There is no discernible pattern in the vibration signatures which could be useful in the interpretation of the acceleration signatures. As such the acceleration signatures may not be useful for condition monitoring of the bearings.

2.2 Displacement Measurements

Though the acceleration signatures could be twice integrated to obtain the displacements of the ends of the viaduct, the above procedure was not adopted. Preliminary work on the double integration of the acceleration signal produced unstable results as the dominant frequency of the dispalcement signature was around 1 Hz.

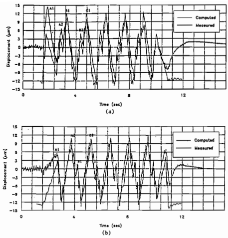

Figure 5. Displacement signatures at (a) x=0, and (b)x=L_s.

Direct measurements of the end movements relative to the columns were made with eddy probes. The eddy probes used were capable of measuring displacement from 0.25 mm to 2.3 mm, producing an output of 20 volts for the above range of displacement. With an initial gap setting of about 1 mm, the steady state outputs from the probes were about 10 volts. The end displacement amplitudes were of the order of 15 μm, giving rise to a variation of 0.12 volt signature superimposed onto the steady state value. As the variation of the displacement signatures was only about 1% of the output, it is desirable to improve on the reliability and accuracy of the output signals obtained.

The outputs from the eddy probes were passed through a high-pass filter with a cut-off frequency at 0.1 Hz. As the largest time interval of the wheels passing through a bearing point was about 1.1 sec, the filter should not have much effect on the output signals from the eddy probes. With the dc value filtered out, the accuracy and reliability of the outut signals from the eddy probes were tremendously improved.

The outputs from the eddy probes after filtering at x=0 and x=L_s were as shown in Fig. 5. Several observations could be made of the displacement signatures. The onset of the movements of the ends of the viaduct was distinct. The duration of the displacement signatures was about 9 sec, the time taken by the train to pass through each bearing location. This shows that the responses of the neighbouring viaducts have very little influence on the end movements of the viaduct under study. There were seven distinct groups, with groups A1, A2, B1, B2, C1, ... corresponding to bogies A1, A2, B1, B2, C1, ... as shown in Fig. 3. During the passage of the train on the viaduct, the peak displacement amplitude of the ends of the viaduct was about 13 μm, compared to less than 1μm when the train was not on the viaduct. The first displacement

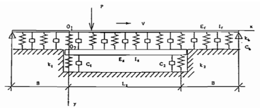

Figure 6. Model for the viaduct system.

peak at $x=L_s$ was about 1 sec later than at $x=0$. This corresponds to the travel time of the first set of wheels to transverse from $x=0$ to $x=L_s$. The displacement patterns showed that the end movements of the viaduct could be used as condition monitoring parameter for the physical condition of the bearings.

3. DYNAMIC RESPONSE OF THE VIADUCT

As shown in Fig.1, the train runs on ballasted track. The viaduct is supported at both ends by bearings mounted on the columns. The viaduct is modelled as shown in Fig. 6 to study its response during a train passage. The viaduct is divided into three sub-systems, namely: (a) the upper beam (the two continuous rails), (b) the elastic foundation (the ballast), and (c) the lower beam (which is the viaduct). The viaduct is supported by bearings which are being modelled by springs and dashpots.

The weight of the total coach (inclusive of the passengers) is assumed to be evenly distributed over the four sets of wheels. The forces acting on the rails are transversing the viaduct with velocity V.

A little digression is in order to complete the assumptions to be made in the above model. For an infinite beam supported on continuous elastic foundation as shown in Fig. 7, the deflection $Y(x)$ due to the point force P acting at $x=0$[2] is given by

$$Y(x) = \frac{P\gamma}{2k_b} e^{-\gamma x}(\cos\gamma x + \sin\gamma x) \tag{1}$$

where k_b is the elastic constant of the foundation and γ is the characteristic of the system and is given by

$$\gamma^4 = \frac{k_b}{4E_rI_r} \tag{2}$$

where E_rI_r is the flexural rigidity of the beam. At $x = 7\pi/4\gamma$, the amplitude of deflection is only 0.4% of the amplitude at $x = 0$, and the total reaction force P' from the foundation between $x = -7\pi/4\gamma$ and $x = +7\pi/4\gamma$ is given by

$$P' = 2\int_0^{\frac{7\pi}{4\gamma}} k_b Y dx = 0.997P \tag{3}$$

Hence for all practical purposes, the effect of the track and viaduct at distance B beyond the ends of the viaduct, where B is set equal to $7\pi/4\gamma$, on the dynamic response of the viaduct can be neglected.

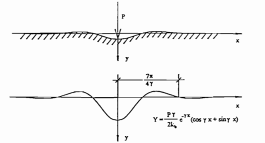

Figure 7. Point load on a beam resting on elastic foundation.

Each point force acting on the track is now given by

$$P(x,t) = P_o\delta(x - Vt) \tag{4}$$

where

$$\delta = 1, \text{ for } x = Vt \text{ and } 0 \le x \le L_r$$
$$= 0, \text{ otherwise.}$$

L_r is taken to be $L_s + 2B$, where the constant B is defined above.

The mode summation method is used to obtain the deflection of the viaduct at $x = 0$ and $x = L_s$. For the upper beam, the origin of the coordinates is at O_1. As the upper beam is assumed to be simply supported at distances B from the ends of the viaduct, the mode shapes of the upper beam are assumed to be sinusoidal:

$$[\Phi_r] = \left[\sin\frac{\pi(x+B)}{L_r}\ \ \sin\frac{2\pi(x+B)}{L_r} \ldots \sin\frac{n_r\pi(x+B)}{L_r}\right] \tag{5}$$

For the lower beam, the origin of the coordinates is at O_2 The lower beam (the viaduct) has the following assumed mode shapes:

$$[\Phi_s] = \left[1 (\frac{L_s}{2} - x) \sin(\frac{\pi x}{L_s})\ \ \sin(\frac{2\pi x}{L_s})\right. \tag{6}$$

where rigid body translation and rotation are permitted. n_r and n_s are integers.

The modal matrix for the overall system can be expressed as:

$$[\Phi] = [\Phi_r\ \Phi_s] \tag{7}$$

The Lagrange's equations can be obtained from

$$\frac{d}{dt}(\frac{\partial T}{\partial \dot{q}_i}) - \frac{\partial T}{\partial q_i} + \frac{\partial U}{\partial q_i} = Q_i \tag{8}$$

where T is the total kinetic energy of the system, U is the total potential energy of the system, and Q_i is the generalized force which is given by the work done δW on the system:

$$\delta W = \sum_{i=1}^{n_r} Q_i\delta q_i = \sum_{i=1}^{n_r} P(x,t)\phi_i\delta q_i \tag{9}$$

where the force $P(x,t)$ acts on the upper beam only. Substituting T, U, and Q_i into Eqn (8), we could obtain the following equations of motion:

$$[M]\{\ddot{q}\}+[C]\{\dot{q}\}+[K]\{q\}=\{Q\} \tag{10}$$

where $[M]$, $[C]$, and $[K]$ are the mass, damping, and stiffness matrices, and $\{Q\}$ are the generalized forces, and

$$\{q\}=\{q_r\, q_s\} \tag{11}$$

where q_r and q_s are the generalized coordinates of the upper and lower beams, respectively. Runge Kutta procedure is used to solve the above equations of motion. The deflection of the lower beam is now given by

$$Y_s(x,t)=[\Phi_s]\{q_s\} \tag{12}$$

4. VIADUCT PARAMETERS USED TO COMPUTE DYNAMIC RESPONSE OF VIADUCT

The following parameters shown in Table 1 are obtained from the constructional details of the viaduct monitored.

Table 1. Available parameters from constructional details.

L_s = 17.2 m	m_r = 121 kg/m (for 2 rails)
m_s = 9895 kg/m	E_r = 200 GPa
E_s = 25 GPa	I_r = 6.1 x 10^{-5} m^4
I_s = 0.529 m^4	m_b = 3850 kg/m

The other parameters required for the computation can be obtained from the characteristics of the train used, and these are:

Mass of empty coach = 14,000 kg.
Maximum number of passengers permitted per coach = 250.
Mass per passenger = 60 kg.
Assuming 50% passenger capacity, P_o = 52,729 N.
Velocity of train at viaduct = 15.9 m/s.

The stiffnesses of the bearings are estimated from the data supplied by the manufacturer and they are:

$$k_1 = k_2 = 8000 \text{ MN/m}.$$

The modulus of the ballast is assumed to be k_b = 900 MN/m^2[3] with damping constant $\varsigma = 0.05$.

The reason for the relatively low velocity is that this viaduct is about 150 m from a station, and that the train has not yet picked up speed then.

With the above parameters, the relative displacements of the ends of the viaduct were computed using Eq (12). The results were found to converge for $n_r = n_s = 5$. These are plotted in Fig 5 as well. Except for the segments of signals when the first set of wheels reached the viaduct and when the last set of wheels left the viaduct, the computed and measured signals are in excellent agreement. As mentioned earlier, in order to improve the accuracy and reliability of the displacement signatures recorded, the outputs from the eddy probes passed through high-pass filters with a cut-off at 0.1 Hz. With and without the train on the viaduct, the equilibrium positions of the viaduct varied, and this change in the equilibrium positions could not be measured with the system as set up. Disregarding the first and last segments of displacement signatures, the results showed that the peak-to-peak dispalcement could be used to condition monitor the physical condition of the bearings.

To examine how effective the end displacements could be used, we note that the following parameters affect the peak-to-peak displacements:

(a) ballast stiffness,
(b) total coach mass, and
(c) bearing stiffnesses.

Due to the regular maintenance of the track system by periodic tamping of the ballast, the modulus of the ballast is not expected to vary significantly. During the off-peak period, the passenger load is estimated to be within 30% to 70% of full capacity.

The next section will examine the sensitivity of the peak-to-peak displacements due to the variations of the above parameters.

5. INFLUENCE OF PARAMETERS ON DISPLACEMENTS

Ballast Stiffness

The nominal stiffness of the ballast used to compute the end displacements of the viaduct is k_b = 900 MN/m. As the ballast is tamped regularly to ensure that the system is running at optimal conditions, we would not expect the ballast stiffness to vary substantially from the nominal value.

Computer simulations have been carried out to determine the percentage changes of the peak-to-peak displacements at $x = 0$ and $x = L_s$ due to the variation of ballast stiffness. The peak-to-peak dispalcements were now represented by Y_1 and Y_2, respectively.

Fig. 8 shows the percentage changes in Y_1 and Y_2 for variation of ballast stiffness from 700 MN/m^2 to 1100 MN/m^2, corresponding to a decrease of 22.2% to an increase of 22.2% over the nominal value. However, the end displacements Y_1 and Y_2 show a variation of less than 1%. This implies that the ballst stiffness has very little influence over the end displacements. This means that condition monitoring by measuring the end diplacements need not necessary be carried out immediately after the tamping operation to ensure a consistent value for the ballast stiffness.

Total Coach Mass

From Eqns (9) and (10), the end displacements are proportional to the imposed load. Hence any change in the total coach mass will produce the corresponding changes in Y_1 and Y_2. As the empty coach mass (14,000 kg) is constant, the variation of the total coach mass is due to the variation in passenger load. Assuming a nominal load of 50% capacity, the total coach mass is 21,500 kg (assuming that each passsenger is of 60 kg). A 30% variation of passenger load (i.e. from 20% to 80% of full capacity), the variation of the total coach mass is ±11%. The corresponding changes in Y_1 and Y_2 are ±11% as shown in Fig. 9.

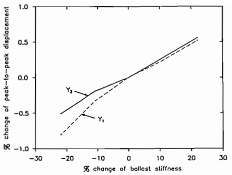

Figure 8. Variations of end displacements with ballast stiffness.

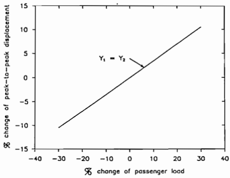

Figure 9. Variations of end displacements with passenger load.

Bearing Stiffnesses - Both Bearings

As there are two sets of bearings for each viaduct, the bearing stiffness could change at either $x = 0$, or $x = L_s$, or at both ends. In this section, we will investigate the effect when bearings at both ends experience the same percentage change in stiffnesses. Fig. 10 shows the variations of Y_1 and Y_2 when the bearings stiffnesses vary from -20% to 100%, i.e., the stiffnesses decrease by 20% to an increase of 100%. For stiffnesses variation of only 12%, Y_1 and Y_2 vary by 11% which is of the same magnitude as 30% variation in passenger load.

When the elastomer ages and deteriorates, the stiffness is expected to increase by more than 50%. The corresponding changes in Y_1 and Y_2 reach 35%, far above that due to the change in passenger load. This shows that by monitoring the end displacements of the viaduct, we could correlate them with the elasticity of the bearings at both ends. When the bearing stiffnesses increase twofold, the end displacement amplitudes reduced to half their amplitudes, a very significant reduction.

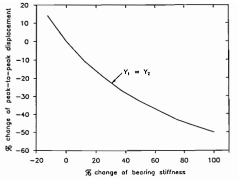

Figure 10. Variations of end displacements due to stiffness changes at both bearings.

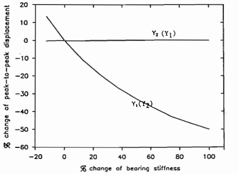

Figure 11. Variations of end displacements due to bearing stiffness change at (a) $x = 0$, and (b) $x = L_s$.

Bearing Stiffness Change at $x = 0$ and at $x = L_s$

Assuming now that only the bearing at $x = 0$ has deteriorated, while that at $x = L_s$ is in good working condition. Fig. 11 shows the changes in Y_1 and Y_2. It can be clearly seen that the displacement at $x = L_s$ is not affected by the deterioration of the bearing at $x = 0$. However, Y_1 varies from +13% to -50% when the bearing stiffness at $x = 0$ varies by -14% to 100%. This clearly shows that the displacement at $x = 0$ is directly affected by the change in bearing stiffness at its support. The variation in Y_1 is about the same regardless of whether the bearing at $x = L_s$ has deteriorated or not. The same observation can be made if the bearing at $x = L_s$ has deteriorated instead of the bearing at $x = 0$. Now only Y_2 will experience a change whereas Y_1 remains the same. These variations are as shown in Fig. 11 (in brackets).

6. CONCLUSION

The above analysis shows that by monitoring the peak-to-peak displacements at both ends of the viaduct, we could correlate the results with the physical properties of the bearings at both ends. The variation of ballast stiffness has very little effect on the displacements. Variation in passengerload of up to 30% would cause at most a 11% change in the peak-to-peak displacements.

Variation of the bearing stiffness by 100% would decrease Y_1 and Y_2 by 50%, a value far above that due to the variation in passenger load. Furthermore, it can be observed that Y_1 would decrease due to an increase in bearing stiffness at $x = 0$, regardless of whether the bearing at $x = L_s$ has deteriorated or not. Similar observation also applies to Y_2. Therefore the end displacements are affected directly by the stiffnesses of the bearings supporting the respective ends.

REFERENCES

1. Long, *Bearings in Structural Engineering,* Newnes-Butterworth (1974).
2. Heteny, M., *Beams on Elastic Foundation,* The University of Michigan Press (1946).
3. Yoder, E. J., and M. W. Witczak, *Principles of Pavement Design John Wiley,* 2nd Edition (1975).